

# Four-wave mixing in photonic crystal waveguides: slow light enhancement and limitations

Juntao Li, Liam O'Faolain, Isabella H. Rey, and Thomas F. Krauss\*

*School of Physics and Astronomy, University of St Andrews, St Andrews, KY16 9SS, UK*

*\*[ffk@st-andrews.ac.uk](mailto:ffk@st-andrews.ac.uk)*

**Abstract:** We demonstrate continuous wave four-wave mixing in silicon photonic crystal waveguides of 396  $\mu\text{m}$  length with a group index of  $n_g = 30$ . The highest observed conversion efficiency is  $-24$  dB for 90 mW coupled input pump power. The key question we address is whether the predicted fourth power dependence of the conversion efficiency on the slowdown factor ( $\eta \approx S^4$ ) can indeed be observed in this system, and how the conversion efficiency depends on device length in the presence of propagation losses. We find that the expected dependencies hold as long as both realistic losses and the variation of mode shape with slowdown factor are taken into account. Having achieved a good agreement between a simple analytical model and the experiment, we also predict structures that can achieve the same conversion efficiency as already observed in nanowires for the same input power, yet for a device length that is 50 times shorter.

©2011 Optical Society of America

**OCIS codes:** (190.4380) Nonlinear optics, four-wave mixing; (130.5296) Photonic crystal waveguides; (260.2030) Dispersion.

---

## References and links

1. T. F. Krauss, "Slow light in photonic crystal waveguides," *J. Phys. D Appl. Phys.* **40**(9), 2666–2670 (2007).
2. T. F. Krauss, "Why do we need slow light?" *Nat. Photonics* **2**(8), 448–450 (2008).
3. T. Baba, "Slow light in photonic crystals," *Nat. Photonics* **2**(8), 465–473 (2008).
4. C. Monat, B. Corcoran, M. Ebnali-Heidari, C. Grillet, B. J. Eggleton, T. P. White, L. O'Faolain, and T. F. Krauss, "Slow light enhancement of nonlinear effects in silicon engineered photonic crystal waveguides," *Opt. Express* **17**(4), 2944–2953 (2009).
5. Y. Hamachi, S. Kubo, and T. Baba, "Slow light with low dispersion and nonlinear enhancement in a lattice-shifted photonic crystal waveguide," *Opt. Lett.* **34**(7), 1072–1074 (2009).
6. K. Inoue, H. Oda, N. Ikeda, and K. Asakawa, "Enhanced third-order nonlinear effects in slow-light photonic-crystal slab waveguides of line-defect," *Opt. Express* **17**(9), 7206–7216 (2009).
7. C. Monat, B. Corcoran, D. Pudo, M. Ebnali-Heidari, C. Grillet, M. D. Pelusi, D. J. Moss, B. J. Eggleton, T. P. White, L. O'Faolain, and T. F. Krauss, "Slow light enhanced nonlinear optics in silicon photonic crystal waveguides," *IEEE J. Sel. Top. Quantum Electron.* **16**(1), 344–356 (2010).
8. B. Corcoran, C. Monat, C. Grillet, D. J. Moss, B. J. Eggleton, T. P. White, L. O'Faolain, and T. F. Krauss, "Green light emission in silicon through slow-light enhanced third-harmonic generation in photonic crystal waveguides," *Nat. Photonics* **3**(4), 206–210 (2009).
9. R. Salem, M. A. Foster, A. C. Turner, D. F. Geraghty, M. Lipson, and A. L. Gaeta, "Signal regeneration using low-power four-wave mixing on silicon chip," *Nat. Photonics* **2**(1), 35–38 (2008).
10. A. Melloni, F. Morichetti, and M. Martinelli, "Four-wave mixing and wavelength conversion in coupled-resonator optical waveguides," *J. Opt. Soc. Am. B* **25**(12), C87–C97 (2008).
11. V. Eckhouse, I. Cestier, G. Eisenstein, S. Combrié, P. Colman, A. De Rossi, M. Santagiustina, C. G. Someda, and G. Vadalà, "Highly efficient four wave mixing in GaInP photonic crystal waveguides," *Opt. Lett.* **35**(9), 1440–1442 (2010).
12. J. F. McMillan, M. Yu, D. Kwong, and C. W. Wong, "Observation of four-wave mixing in slow-light silicon photonic crystal waveguides," *Opt. Express* **18**(15), 15484–15497 (2010).
13. C. Monat, M. Ebnali-Heidari, C. Grillet, B. Corcoran, B. J. Eggleton, T. P. White, L. O'Faolain, J. Li, and T. F. Krauss, "Four-wave mixing in slow light engineered silicon photonic crystal waveguides," *Opt. Express* **18**(22), 22915–22927 (2010).
14. K. Suzuki, and T. Baba, "Nonlinear light propagation in chalcogenide photonic crystal slow light waveguides," *Opt. Express* **18**(25), 26675–26685 (2010).

15. S. A. Schulz, L. O'Faolain, D. M. Beggs, T. P. White, A. Melloni, and T. F. Krauss, "Dispersion-engineered slow light in photonic crystals: A comparison," *J. Opt.* **12**(10), 104004 (2010).
16. J. Li, T. P. White, L. O'Faolain, A. Gomez-Iglesias, and T. F. Krauss, "Systematic design of flat band slow light in photonic crystal waveguides," *Opt. Express* **16**(9), 6227–6232 (2008).
17. A. Petrov, M. Krause, and M. Eich, "Backscattering and disorder limits in slow light photonic crystal waveguides," *Opt. Express* **17**(10), 8676–8684 (2009).
18. M. Patterson, S. Hughes, S. Schulz, D. M. Beggs, T. P. White, L. O'Faolain, and T. F. Krauss, "Disorder-induced incoherent scattering losses in photonic crystal waveguides: Bloch mode reshaping, multiple scattering, and breakdown of the Beer-Lambert law," *Phys. Rev. B* **80**(19), 195305 (2009).
19. S. J. McNab, N. Moll, and Y. A. Vlasov, "Ultra-low loss photonic integrated circuit with membrane-type photonic crystal waveguides," *Opt. Express* **11**(22), 2927–2939 (2003).
20. S. G. Johnson, and J. D. Joannopoulos, "Block-iterative frequency-domain methods for Maxwell's equations in a planewave basis," *Opt. Express* **8**(3), 173–190 (2001).
21. T. Tanabe, M. Notomi, S. Mitsugi, A. Shinya, and E. Kuramochi, "All-optical switches on a silicon chip realized using photonic crystal nanocavities," *Appl. Phys. Lett.* **87**(15), 151112 (2005).
22. G. P. Agrawal, *Nonlinear Fiber Optics*, 2nd ed. (Academic Press, 1995).
23. L. O'Faolain, S. A. Schulz, D. M. Beggs, T. P. White, M. Spasenović, L. Kuipers, F. Morichetti, A. Melloni, S. Mazoyer, J. P. Hugonin, P. Lalanne, and T. F. Krauss, "Loss engineered slow light waveguides," *Opt. Express* **18**(26), 27627–27638 (2010).

---

## 1. Introduction

Using slow light to enhance nonlinear effects in planar waveguide structures has recently developed into a very promising concept in Photonics. By controlling the effective speed of propagation of optical waveguide modes, one can increase the energy density in the waveguide and thus enhance the light-matter interaction [1–3]. Such slow light enhancement has already been demonstrated in photonic crystal (PhC) waveguides for many third-order susceptibility ( $\chi^{(3)}$ ) nonlinear processes such as self-phase modulation [4–7], third-harmonic generation [7,8], and four-wave mixing (FWM) [9–14].

The process of FWM [9,10] can be used in many functional integrated optical devices, for example in optical regenerators [9]. Slow light adds an important control parameter to enhance this effect. Ideally, the FWM process scales with the fourth power of the slowdown factor ( $S^4$ ) if all four waves are slowed down equally. Several researchers have already observed the enhancement of the FWM process in the slow light regime [11–14], but the predicted  $S^4$  dependence has not yet been observed, which may be due to effects such as group velocity dispersion (GVD), propagation losses and mode shape variation.

Let us examine these constraints. The strong dispersion of slow light in PhC waveguides can cause phase mismatch issues that result in a narrow bandwidth of less than 1 or 2 nm for the FWM process as well as substantially degrading the conversion efficiency [11,12]. Dispersion engineered PhC waveguides with flat band and low dispersion slow light can overcome this problem, however [13,14]. A typical slowdown factor of 10-20 (group index 30 - 60) combined with low dispersion can be achieved over a bandwidth of 7 - 15 nm in the 1550 nm region with such engineered silicon PhC waveguides [15,16]. Using dispersion engineered waveguides allows us to enhance all four waves by the same slowdown factor and to compensate phase mismatch effects. The next limitation is propagation loss. As already pointed out by Melloni et al. [10], the conversion process is rather sensitive to losses, thus limiting practical devices to relatively short lengths. Additionally, it has recently been recognized [17,18] that the mode size increases as a function of group index, thus reducing the effective nonlinear parameter. By taking all of these effects into account, we develop a modified  $S^4$  enhancement formula and demonstrate good agreement with experimental values.

## 2. Fabrication and the experimental setup

We fabricated 396  $\mu\text{m}$  long engineered slow light ( $n_g = 30$ ) silicon PhC waveguides [16] with on-chip inverse taper mode converters [19] for enhanced injection efficiency. The waveguides were fabricated on a SOITEC Silicon on Insulator wafer by electron beam lithography [15] (Fig. 1 (a)), and they exhibited a constant group index of  $n_g = 30$  with a 13 nm bandwidth around 1550 nm (Fig. 1 (b)). The linear propagation loss in the slow light region was estimated from cutback measurements to be 65 dB/cm. The group velocity dispersion (GVD)

was  $0.6 \times 10^{-21} \text{ s}^2/\text{m}$ , as calculated from the 3D plane-wave expansion method [20]. This GVD value is sufficiently low to maintain phase matching of the FWM process for the 396  $\mu\text{m}$  long sample [13]. The inverse taper has a length of 100  $\mu\text{m}$  and a tip of 100 nm width at the end. It is fed from a  $5.5 \mu\text{m} \times 2 \mu\text{m}$  SU8 polymer waveguide that acts as the spot size mode converter [19]. The large cross-sectional area of the polymer waveguide avoids issues with facet damage that can occur for high continuous wave (cw) pump power. This relatively large cross-section of the polymer waveguide makes a high coupling efficiency more difficult to achieve, hence we only measure about 38% injection efficiency for the coupler.

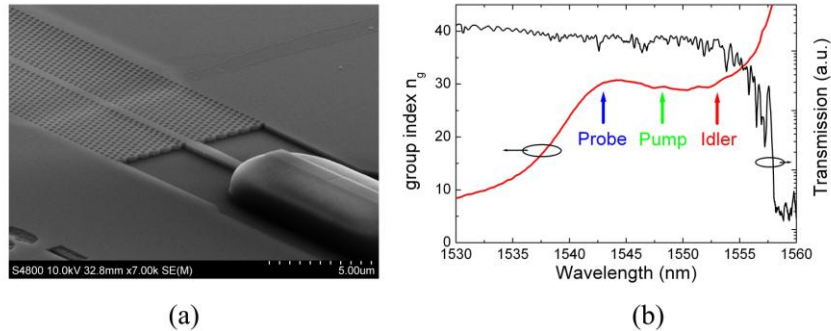


Fig. 1. (a) Scanning electron micrograph (SEM), (b) Measured transmission spectrum (black) and group index (red) of the engineered slow light PhC waveguide with spot size mode converter. The arrows in (b) indicate the spectral position of the pump, probe and idler.

We used a degenerate pump configuration for the FWM process. As shown in Fig. 2, a tunable cw laser was amplified by an EDFA ( $P_{\text{max}} = 600 \text{ mW}$ ) and acted as the pump. A cw polarization maintaining DFB laser diode of 60 mW was added to the beampath via a 50:50 beamsplitter cube and acted as the signal probe. The polarization of the pump laser is controlled by quarter- and half-wave plates (WP1, WP2) in order to achieve a TE input into the waveguide. Given the 38% coupling efficiency and  $\sim 60\%$  loss from the beamsplitter, wave plates and polarizer, we estimated a maximum coupled pump power of 90 mW and probe power of 9 mW. The output light of the waveguide was collected by two microscope objectives and fed into an optical spectrum analyzer (OSA).

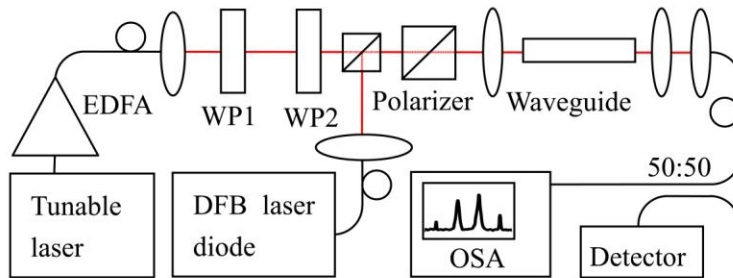


Fig. 2. Schematic setup of the FWM experiment. WP1 and WP2 are quarter- and half-wave plates, respectively, that are used to control the polarization of the cw pump laser.

### 3. Results

The experimental data is shown in Fig. 3, for a coupled cw pump at 1551 nm and a coupled cw probe at 1550 nm. The corresponding idler signal was observed around 1552 nm as expected. As indicated in Fig. 1(a), all three pump, probe and idler waves were positioned in the flat band slow light region to ensure uniform enhancement. The FWM conversion efficiency, which is defined as the ratio between idler power on the output side and the probe power on the input side of structure, was  $-24 \text{ dB}$ . To our knowledge, this is the highest cw

conversion efficiency in PhC waveguides observed to date. Furthermore, up to 6 nm pump-probe detuning of the FWM efficiency was observed (inset of Fig. 3), which is much wider than that observed with non-dispersion engineered PhC waveguides [11,12].

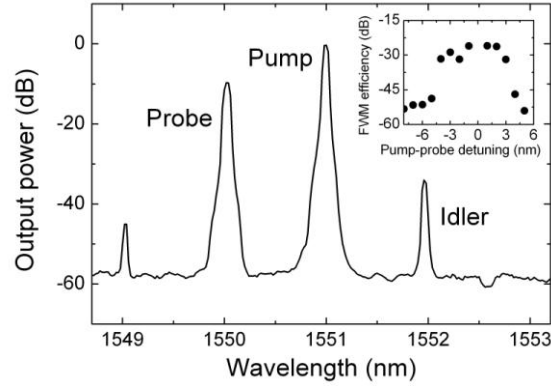


Fig. 3. Measured FWM spectra from the slow light PhC waveguide. The coupled cw pump power was 90 mW at 1551 nm and the coupled cw probe power was 9 mW at 1550 nm. Inset: FWM efficiency dependence on pump-probe detuning. The pump wavelength was tuned while the probe wavelength was kept constant at 1550 nm.

The carrier lifetime in the silicon PhC waveguides ( $\approx 100$  ps) [21] is typically one order of magnitude shorter than in silicon nanowires. For cw operation, this means that the saturation power caused by the nonlinear loss is above 100 mW, even for the case of  $n_g = 60$  and 400  $\mu\text{m}$  long waveguides. Furthermore, the saturation power can increase up to 1W for the pulsed case [13]. Hence we can ignore nonlinear losses in the rest of the discussion. Thus, the FWM conversion efficiency  $\eta$  can be expressed as [9,13,20]:

$$\eta = \frac{P_{\text{idler}}(L)}{P_{\text{probe}}(0)} = S^4 \gamma^2 \bar{P}_{\text{pump}}^2 L^2 e^{-\alpha L} \varphi, \quad (1)$$

where  $S$  is the slowdown factor,  $\gamma = 2\pi n_{2\text{eff}} / (\lambda \cdot A_{\text{eff}})$  is the material nonlinear parameter,  $n_{2\text{eff}} = 5 \times 10^{-18} \text{ m}^2 / \text{W}$  is the effective nonlinear index of silicon [7],  $A_{\text{eff}}$  is the effective cross-section mode area [7,22],  $\bar{P}_{\text{pump}} = P_{\text{pump}}(0) \times (1 - \exp(-\alpha L)) / \alpha L$  is the path average pump power,  $\alpha$  and  $L$  are the loss and physical length of the structure, and  $\varphi$  is the phase factor. As already discussed in [13], the phase mismatching in our engineered PhC waveguides is negligible in the flat band slow light region due to its low GVD. Hence we can also ignore the phase mismatching effect in the rest of the paper unless stated otherwise.

In order to verify the validity of Eq. (1), we tested three different types of waveguides, namely an engineered slow light silicon PhC waveguide with a group index of  $n_g = 30$ , a standard silicon PhC waveguide with a group index of  $n_g = 10$  and a silicon nanowire of the same length with a group index of  $n_g = 4$ , the length (396  $\mu\text{m}$ ) being determined by multiples of the writefield used in the e-beam lithography process (100  $\mu\text{m}$ ). The experimental FWM conversion efficiency for these three structures as a function of the coupled input pump power is shown in Fig. 4, together with a comparison with the values expected from Eq. (1). In the calculation, we used effective mode areas of 0.5  $\mu\text{m}^2$ , 0.25  $\mu\text{m}^2$  and 0.12  $\mu\text{m}^2$  derived from MPB [20] calculations, and propagation losses of 65 dB/cm, 20 dB/cm and 2 dB/cm derived from cut-back measurements for  $n_g = 30$ , 10 and 4, respectively. We note that the experimental signals are slightly larger than the calculated ones, which we relate to the FWM contribution of the silicon inverse taper.

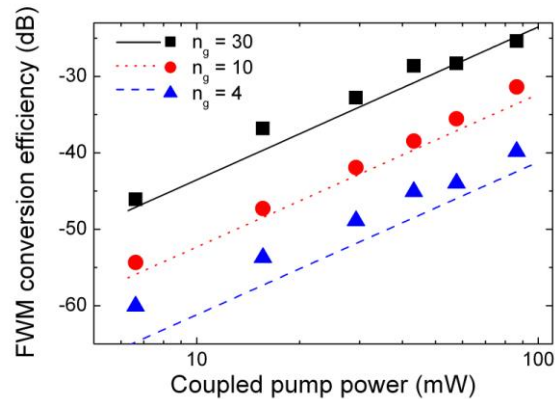


Fig. 4. Comparison of the FWM conversion efficiency vs. the coupled input pump power in an engineered slow light PhC waveguide ( $n_g = 30$ , black), a standard PhC waveguide ( $n_g = 10$ , red), and a nanowire ( $n_g = 4$ , blue) of same length (396  $\mu\text{m}$ ). Dots and lines represent the experimental and calculated results according to Eq. (1), respectively.

Figure 4 shows the conversion efficiency as a function of input power for the three different structures. Firstly, we note that all the curves are linear up to the maximum coupled power of 90 mW, which indicates that there is indeed no noticeable nonlinear loss and the omission of nonlinear loss terms from Eq. (1) is justified. Secondly, the curves allow us to compare the observed efficiency to the expected  $S^4$  dependence. In the ideal, lossless case, we would expect an enhancement of 35 dB by increasing the slowdown factor from  $n_g = 4$  to  $n_g = 30$ . By taking the mode shape variation into account, this value drops to 23 dB, and further to 17.5 dB with losses. The experimentally observed value is 15 dB, which is in good agreement given experimental uncertainties and the fact that some FWM conversion may occur in the inverse tapers. This comparison highlights the somewhat surprising fact that the mode shape variation, which leads to an increase in the mode size by a factor 4 between the nanowire and the slow light PhC, is the main reason for the large deviation between the expected  $S^4$  dependence and the experimentally observed conversion efficiencies.

Figure 4 confirms the strong enhancement of the FWM process available in slow light waveguides and explains it quantitatively. The next step is to use the good agreement of the experimental data with Eq. (1) in order to predict further improvements. As a useful yardstick, we chose to compare our results with those available in silicon nanowires, where a conversion efficiency of  $-11.7$  dB was reported for similar input power as here, but for much longer (18 mm) waveguides [9]. If a similar conversion efficiency as in nanowires can be obtained with slow light waveguides, then their much reduced size offers real advantages for integration. Figure 5 gives an example for such a waveguide and puts it into perspective by plotting the relationship between waveguide length and FWM conversion efficiency for a number of structures with different group indices and losses. Dots and lines represent the experimental and calculated results. The ideal  $S^4$  and  $L^2$  enhancement of the FWM efficiency in a lossless sample, taking the mode shape into account, is plotted as the dark green dotted line for  $n_g = 30$ . By adjusting for realistic losses of 65 dB/cm (black solid line in Fig. 5), the maximum conversion efficiency is limited by the waveguide length, even before phase mismatch issues becomes important (we estimate from the GVD value that phase mismatch effects occur for lengths  $L > 1$  mm); the conversion efficiency peaks for  $L = 600\text{-}800\mu\text{m}$ , which is not surprising as this corresponds to the decay length of the pump. Further improvements can be obtained by reducing the loss [23], thus enabling longer devices (dark gray dashed line in Fig. 5) or by increasing the group index (blue dash-dotted line in Fig. 5). We have already been able to simulate devices with  $n_g = 60$  and 90 dB/cm loss using the new concept of “loss engineering” [23], which has the same effective mode area as the  $n_g = 30$  waveguide according to our calculation. We expect to achieve the same FWM conversion efficiency as in

the silicon nanowire (~12 dB) (red dotted line in Fig. 5) by using this design for the same pump power but with 50 times shorter devices.

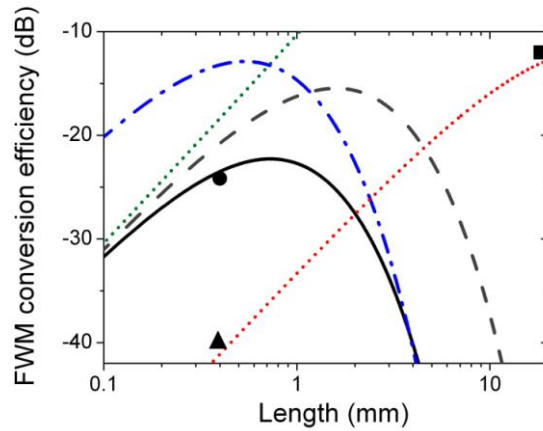


Fig. 5. Relationship between the waveguide length and the FWM conversion efficiency for different silicon structures as a function of the group index with 100 mW coupled pump power; a) Slow light with  $n_g = 30$ , no loss (dark green dotted line); b) Slow light with  $n_g = 30$  and 65 dB/cm loss (black solid line); c) Slow light with  $n_g = 30$  and 30 dB/cm loss (dark gray dashed line); d) Slow light with  $n_g = 60$  and 90 dB/cm loss (blue dash-dotted line); e) Nanowire with  $n_g = 4$  and 1.5 dB/cm loss (red dotted line). The circle indicates the experimental result from Fig. 3 (-24 dB FWM efficiency with  $n_g = 30$ , 65 dB/cm loss and 90 mW pump power), the triangle indicates the nanowire result from Fig. 4 (-40 dB FWM efficiency with group index  $n_g = 4$ , 2 dB/cm loss and 90 mW pump power), and the square indicates the nanowire result reported in [9] (-11.7 dB FWM efficiency with group index  $n_g = 4$ , 1.5 dB/cm loss and 100 mW pump power).

#### 4. Conclusion

In conclusion, by using dispersion engineered slow light silicon PhC waveguides, we have been able to demonstrate the highest cw FWM conversion efficiency in PhC waveguides (-24 dB, 90 mW pump) reported to date, for waveguides as short as 396  $\mu\text{m}$ . The flat band dispersion engineering allows for a pump-probe detuning bandwidth of 6 nm. The result is in good agreement with a simple analytical model, which highlights the fact that the performance is limited by both the mode shape (mode shape increases 4-fold in an  $n_g = 30$  PhC waveguide compared to a nanowire) and the loss (loss limits the waveguide length to  $L < 1$  mm). Mode shape and loss are the key constraints for obtaining the  $S^4$  enhancement that is expected in the ideal case, while we believe that dispersive effects and nonlinear losses are not an issue in these waveguides. As a result, we predict that by reducing the loss and increasing the group index to realistic values, a conversion efficiency approaching -10 dB can be achieved. Such a high conversion efficiency has already been reached with nanowires, but the slow light approach would realise this performance in a much more compact geometry and therefore enable much tighter integration, as required e.g. for multichannel optical signal processing. Ultimately, further improvements should then enable the pump power to be reduced, thus realising the dream of truly low power nonlinear optics.

#### Acknowledgement

This work was supported by the EPSRC - UK Silicon Photonics consortium. Dr. J. Li was supported by EU-FP7 Marie Curie Fellowship project "OSIRIS". The fabrication was carried out in the framework of NanoPix ([www.nanophotonics.eu](http://www.nanophotonics.eu)).